Polarimetric radar sounding methods to characterise ice birefringence, fabric anisotropy, and flow history

TJ Young Scott Polar Research Institute

Tom Jordan Plymouth Marine Laboratory

Carlos Martín British Antarctic Survey

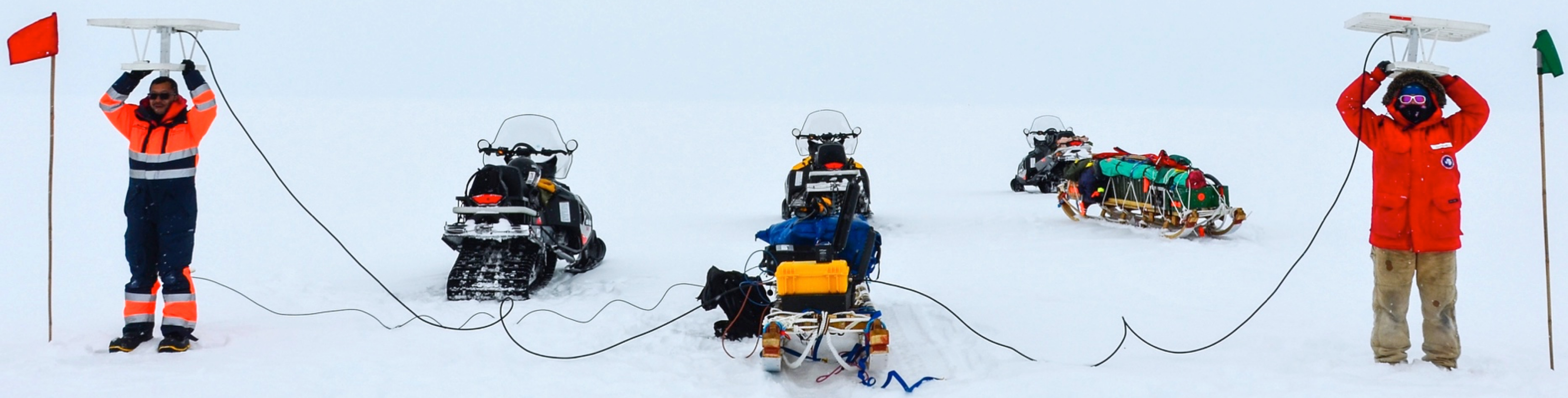

What is ice fabric?

- Ice fabric represents the collective orientations of ice crystals
- Represented by a 2nd order orientation tensor with eigenvalues *a* along eigenvectors *x*:

  $a_1 + a_2 + a_3 = 1$

  $a_1 < a_2 < a_3$ (radar, seismics)

  $a_1 > a_2 > a_3$ (ice cores)

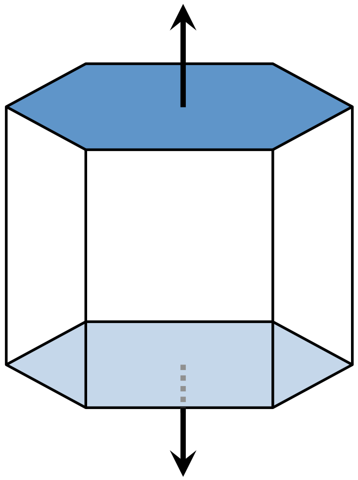

The *c*-axis of a single ice crystal

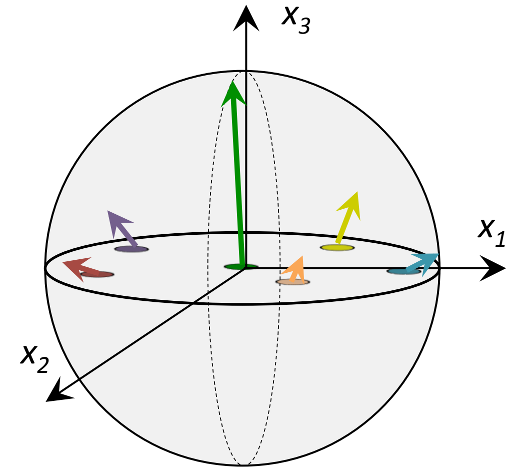

<u>Ice fabric</u>: *c*-axes of *many* ice crystals

Fabric anisotropy

- Fabric represents the deformation history of glacier ice
- “Complex history → complex fabric”

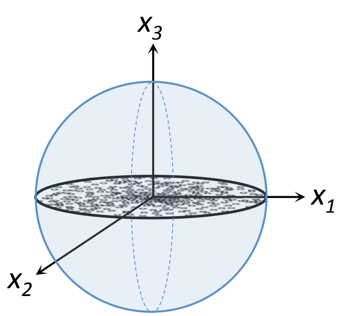

Isotropic (near-random)
$a_1 \approx a_2 \approx a_3 \approx 1/3$
Near-surface firn/ice
Uniform deformation

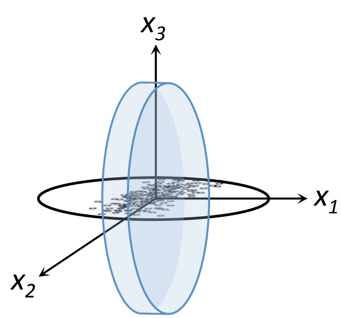

Vertical girdle
$a_1 << a_2 \approx a_3$
Centre of glacier
Uniaxial compression, longitudinal extension

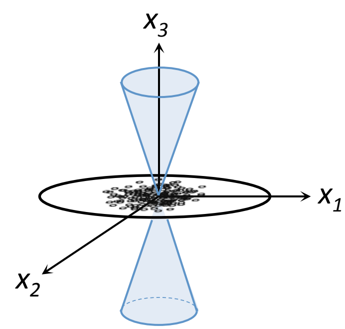

Vertical cluster
$a_1 \approx a_2 << a_3$
Near-bed ice
Planar simple shear

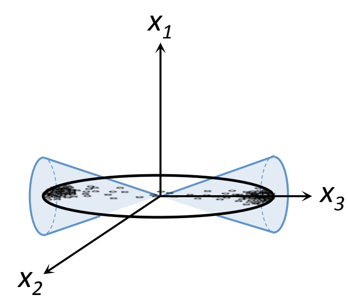

Horizontal cluster
$a_1 \approx a_2 << a_3$
Glacier shear margin
Lateral simple shear

Further reading

Azuma & Higashi (1985) AoG
Alley (1988) Nature

* Shown are *general* examples (deviations occur!)

Birefringence in ice

Radar is able to detect the horizontal components of fabric anisotropy due to the birefringence of ice as an effective medium

$$\varepsilon = \begin{bmatrix} \varepsilon_x & 0 & 0 \\ 0 & \varepsilon_y & 0 \\ 0 & 0 & \varepsilon_z \end{bmatrix}$$

$$= \begin{bmatrix} \varepsilon_\perp + a_1\Delta\varepsilon' & 0 & 0 \\ 0 & \varepsilon_\perp + a_2\Delta\varepsilon' & 0 \\ 0 & 0 & \varepsilon_\perp + a_3\Delta\varepsilon' \end{bmatrix}$$

$$\Delta\varepsilon = \varepsilon_y - \varepsilon_x = (a_2 - a_1)\,\Delta\varepsilon'$$

This equation relates the bulk (macroscopic) birefringence $\Delta\varepsilon$ to the microscopic (crystal) birefringence $\Delta\varepsilon'$

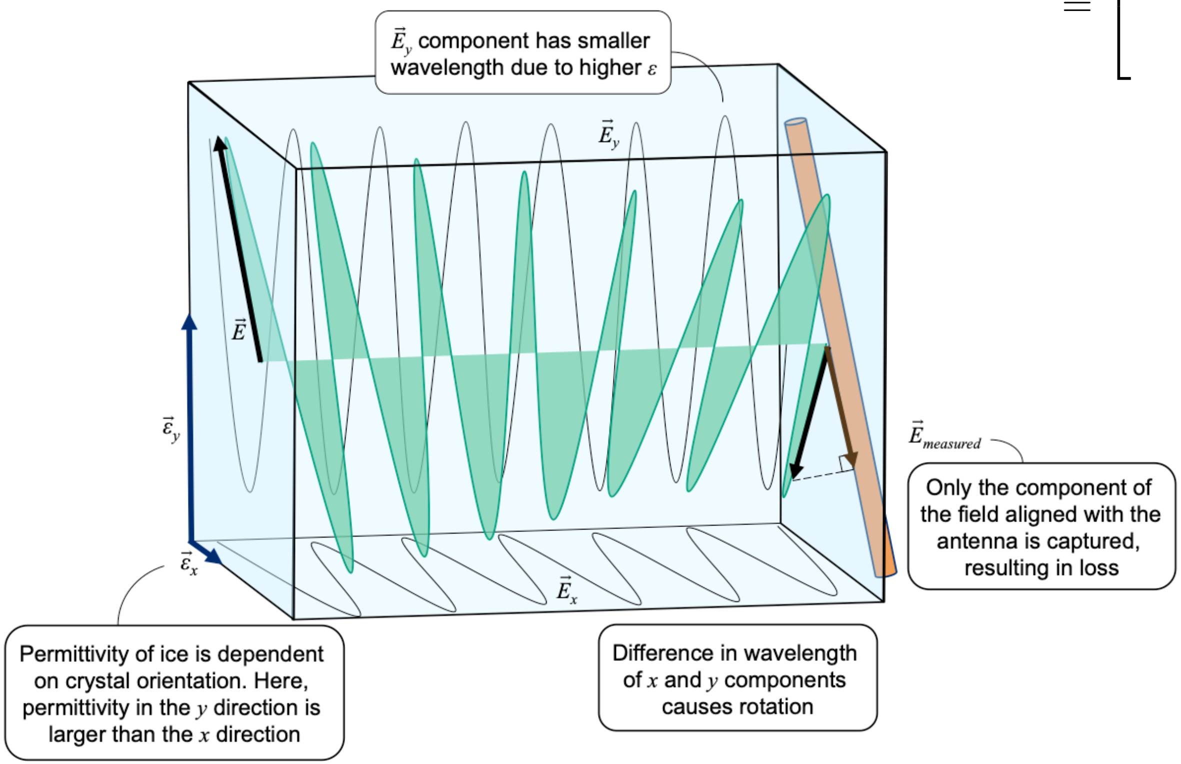

Further reading

Hargreaves (1978) JGlac
Doake (1981) GJI
Fujita et al. (2006) JGlac
Young et al. (*in review*) JGR

Birefringence in ice

- In radargrams, periodic patterns appear as a result of birefringence
- Radar must be angled off-parallel and off-perpendicular to fabric axes!

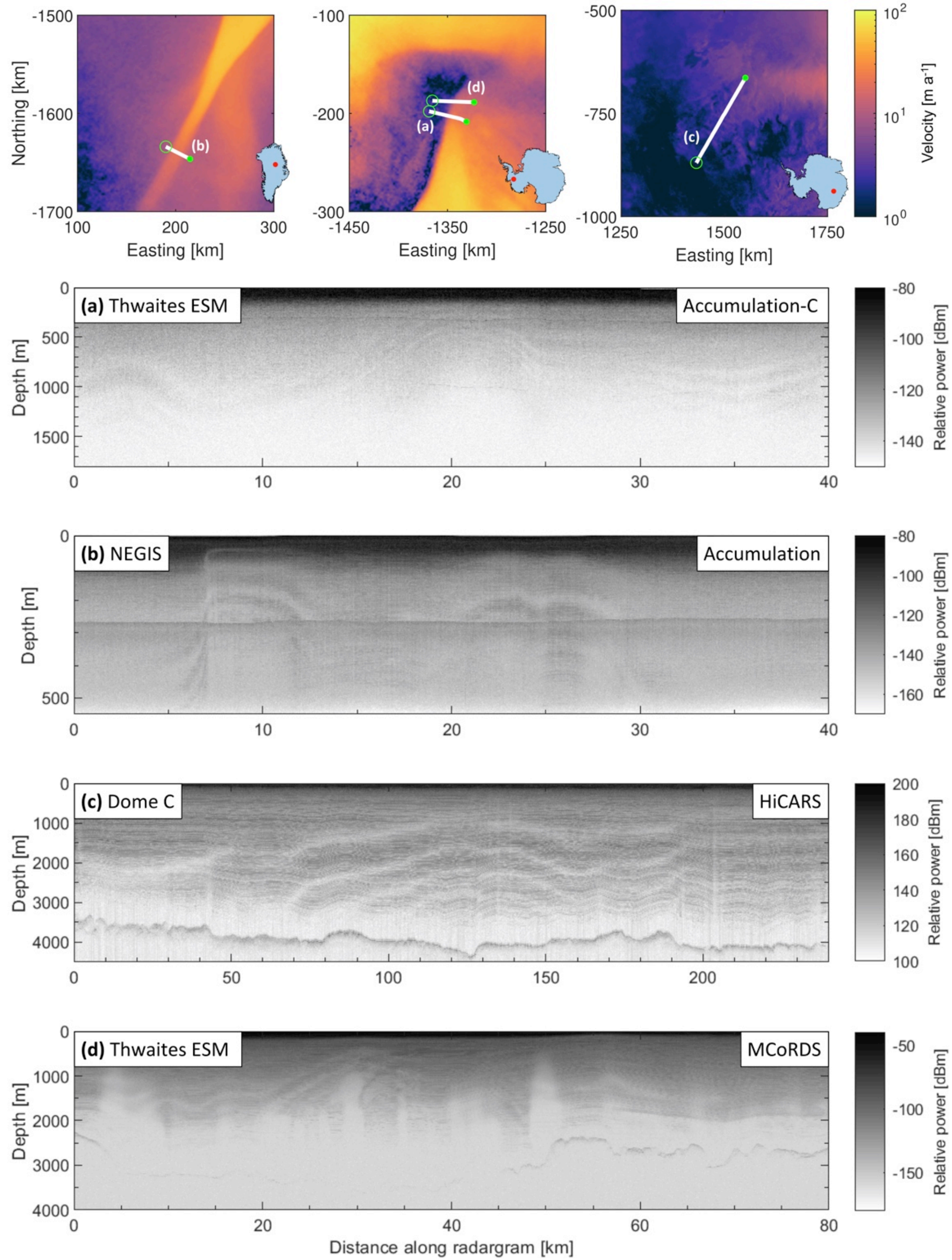

Further reading: Young et al. (*in review*) JGR

Polarimetric backscatter model

$$S(\theta) = \left[\frac{\exp(jk_0 z)}{4\pi z}\right]^2 \cdot \left[\prod_{i=1}^{N} (RTR')_{\theta,\varepsilon,N+1-i}\right] \cdot [R\Gamma R']_{\theta,\beta,N} \cdot \left[\prod_{i=1}^{N} (RTR')_{\theta,\varepsilon,i}\right]$$

free-space propagation | received (upward) propagation | boundary scattering | transmitted (downward) propagation

$$T = \begin{bmatrix} T_x & 0 \\ 0 & T_y \end{bmatrix}$$

$$R = \begin{bmatrix} \cos\theta & \sin\theta \\ -\sin\theta & \cos\theta \end{bmatrix}$$

$$\Gamma = \begin{bmatrix} r & 0 \\ 0 & 1 \end{bmatrix}$$

Node azimuth separation dependent on anisotropic scattering (*r*)

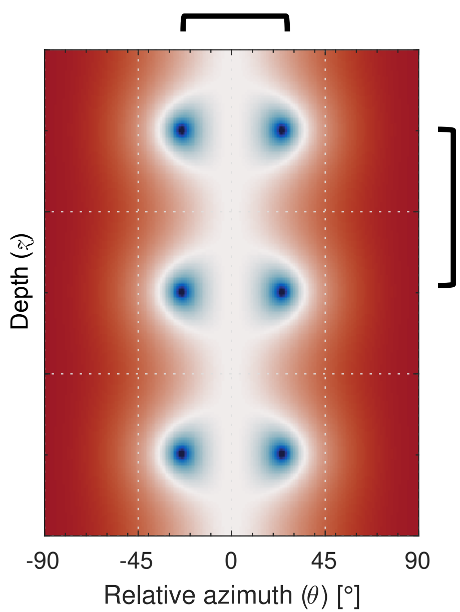

Node depth wavelength (ϕ) dependent on:

- frequency (f_c),
- bulk birefringence ($\Delta\varepsilon(z)$)
- crystal birefringence (through ε)

$$\phi = \frac{4\pi f_c}{c} \int_{z_0}^{z} \frac{\Delta\varepsilon(z)}{2\sqrt{\bar{\varepsilon}}} dz$$

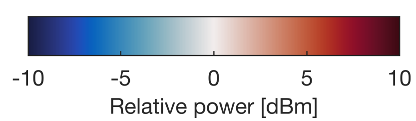

Further reading

Fujita et al. (2006) JGlac

Young et al. (*in review*) JGR

Polarimetric radar sounding

Application to radar sounding using <u>linearly-polarised antennas</u> can detect azimuthal (*x*-*y*) fabric asymmetry

$$S(\theta) = \begin{bmatrix} \cos\theta & \sin\theta \\ -\sin\theta & \cos\theta \end{bmatrix} \begin{bmatrix} s_{hh} & s_{vh} \\ s_{hv} & s_{vv} \end{bmatrix} \begin{bmatrix} \cos\theta & -\sin\theta \\ \sin\theta & \cos\theta \end{bmatrix}$$

$$= \begin{bmatrix} s_{hh}\cos^2\theta + (s_{vh}+s_{hv})\sin\theta\cos\theta + s_{vv}\sin^2\theta & s_{hv}\cos^2\theta + (s_{vv}-s_{hh})\sin\theta\cos\theta - s_{vh}\sin^2\theta \\ s_{vh}\cos^2\theta + (s_{vv}-s_{hh})\sin\theta\cos\theta - s_{hv}\sin^2\theta & s_{vv}\cos^2\theta - (s_{vh}+s_{hv})\sin\theta\cos\theta + s_{hh}\sin^2\theta \end{bmatrix}$$

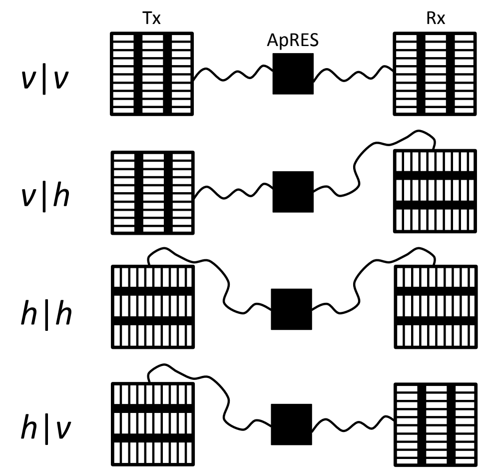

Quad-pol setup

Modelled

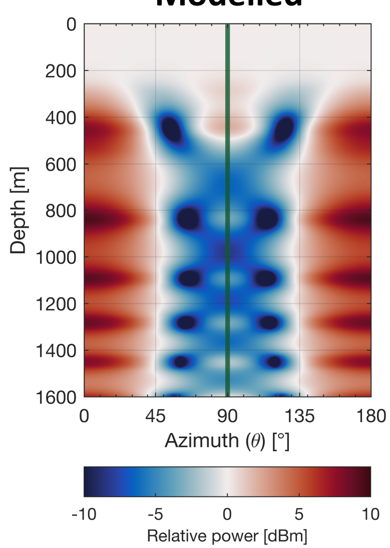

Measured

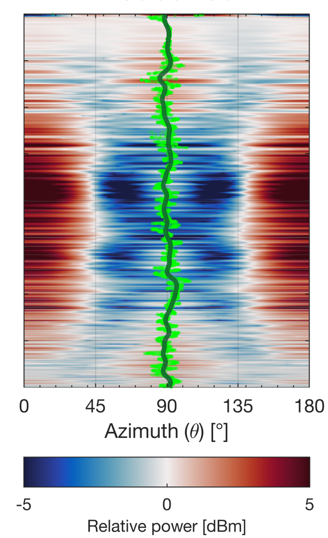

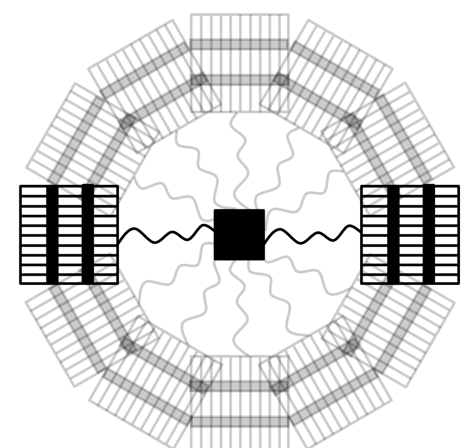

Azimuthal rotation setup

Further reading

Brisbourne et al. (2019) JGR
Young et al. (2020) TCD

Polarimetric coherence

Application of polarimetric coherence to the effective medium model quantifies the azimuthal fabric asymmetry

$$c^{\star}_{hhvv} = \frac{\sum_{i=1}^{N} s_{hh,i} \cdot s^{*}_{vv,i}}{\sqrt{\sum_{i=1}^{N} |s_{hh,i}|^2}\sqrt{\sum_{i=1}^{N} |s_{vv,i}|^2}}$$

$$\phi^{\star}_{hhvv} = \arg\left(c_{hhvv}\right)$$

$$a_2 - a_1 = \frac{c}{4\pi f_c}\frac{2\sqrt{\bar{\varepsilon}}}{f(\nu)\Delta\varepsilon'}\left|\frac{d\phi_{hhvv}}{dz}\right|$$

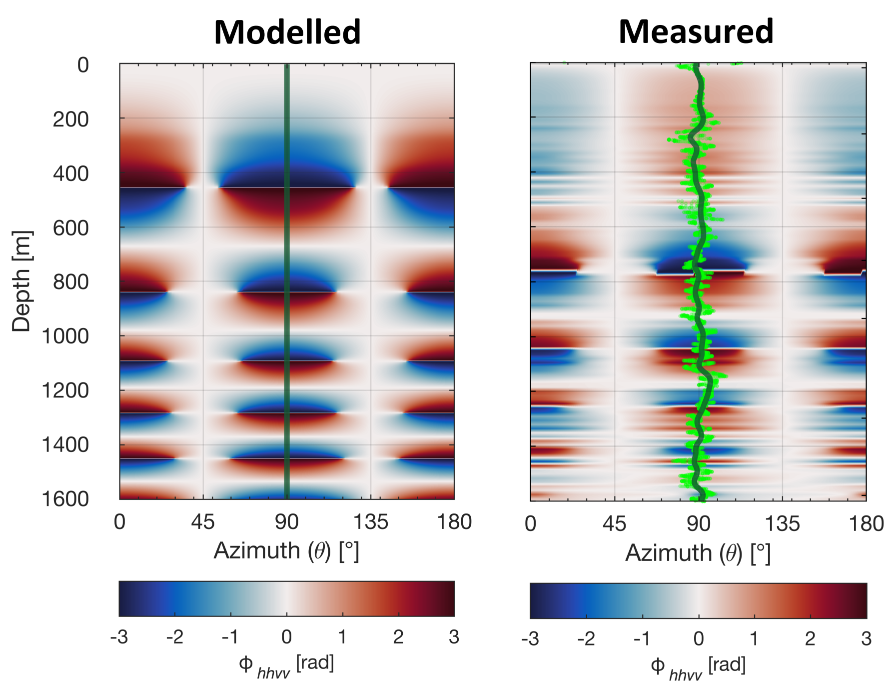

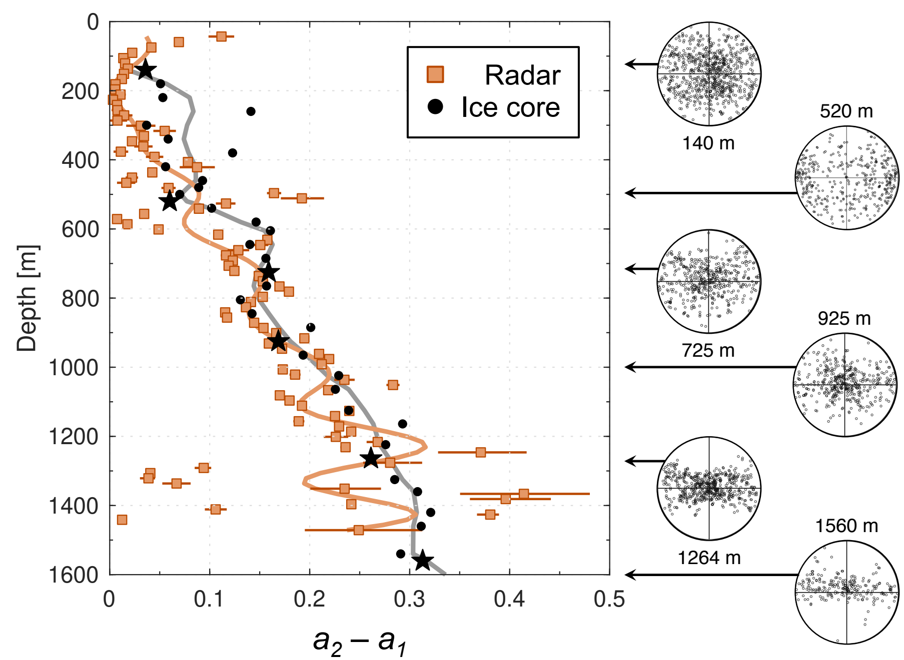

Further reading: Young et al. (2020) TCD

Application: Thwaites Glacier

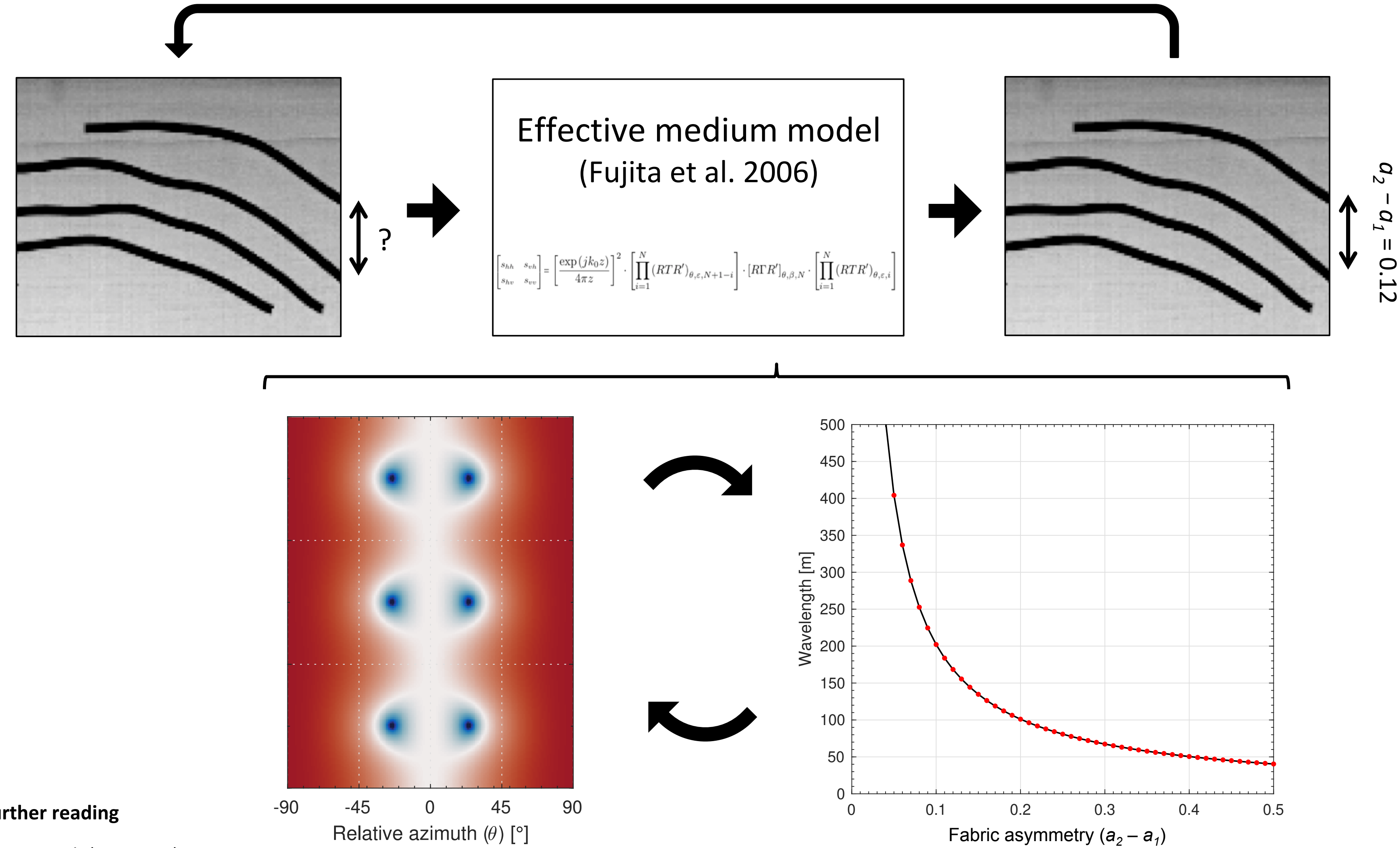

$$\begin{bmatrix} s_{hh} & s_{vh} \\ s_{hv} & s_{vv} \end{bmatrix} = \left[\frac{\exp(jk_0 z)}{4\pi z}\right]^2 \cdot \left[\prod_{i=1}^{N} (RTR')_{\theta,\varepsilon,N+1-i}\right] \cdot [R\Gamma R']_{\theta,\beta,N} \cdot \left[\prod_{i=1}^{N} (RTR')_{\theta,\varepsilon,i}\right]$$

Further reading

Young et al. (*in review*) JGR

Application: Thwaites Glacier

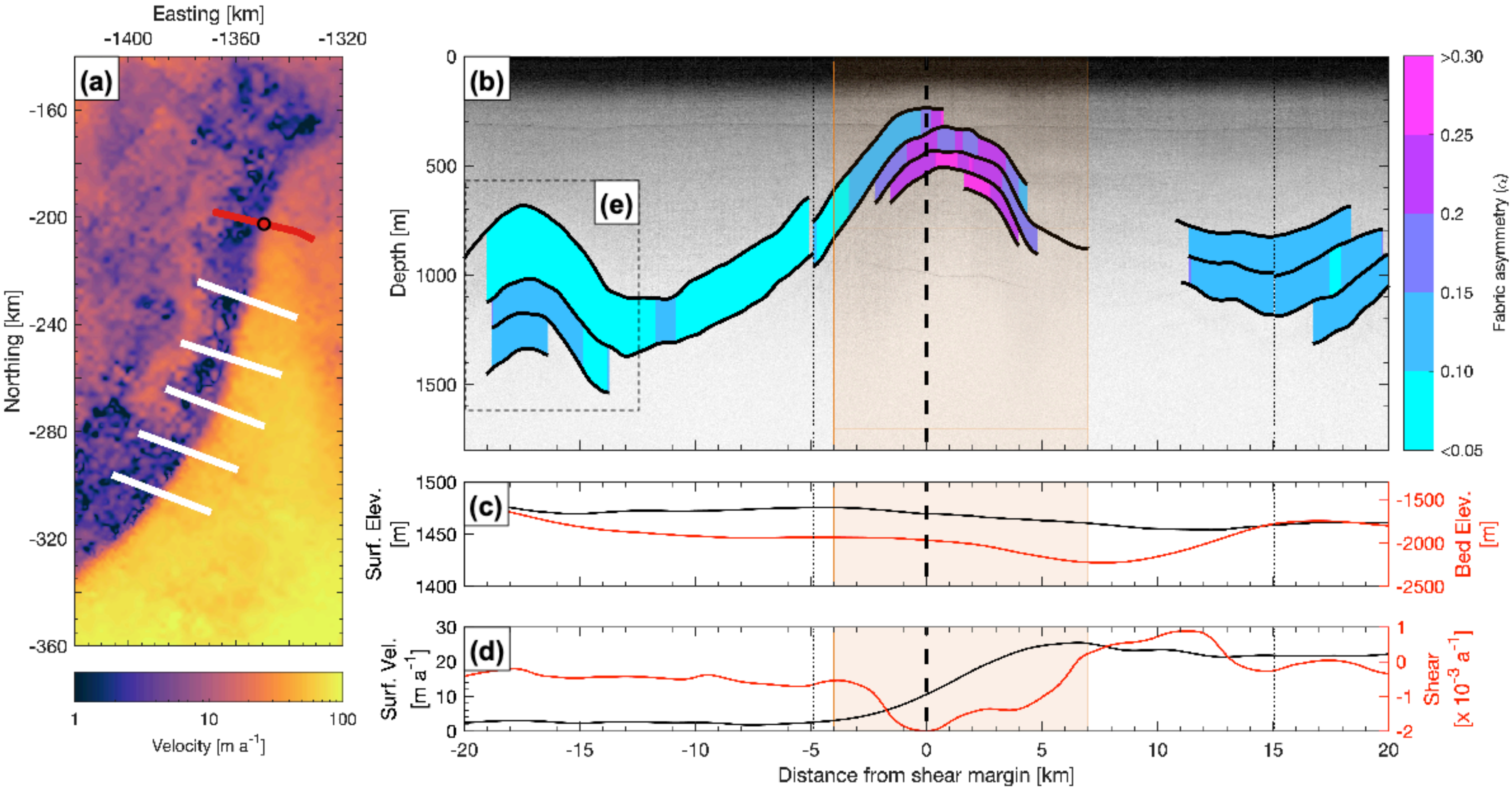

Further reading: Young et al. (*in review*) JGR

Application: Rutford Ice Stream

pRES observations approaching the shear margin of Rutford Ice Stream reveals increasing fabric asymmetry and axis rotation

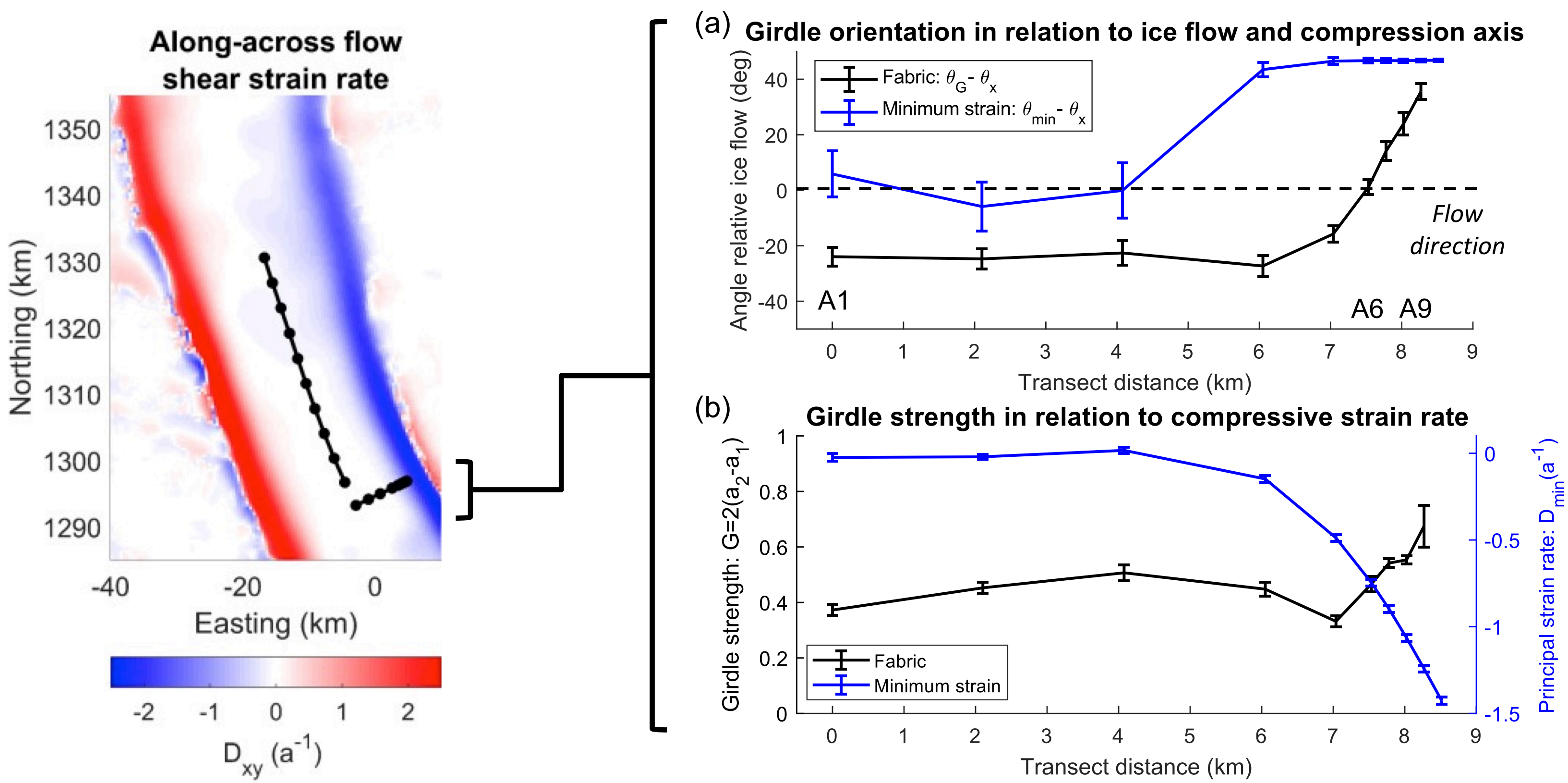

Further reading: Jordan et al. (*in review*) JGR

Application: Rutford Ice Stream

Radar fabric measurements can be used to parameterise an anisotropic flow law via the fluidity tensor ψ

$$\begin{pmatrix} D_{11} \\ D_{22} \\ D_{33} \\ D_{12} \\ D_{13} \\ D_{23} \end{pmatrix} = \psi_0 \begin{pmatrix} \psi_{1111} & \psi_{1122} & \psi_{1133} & 0 & 0 & 0 \\ \psi_{1122} & \psi_{2222} & \psi_{2233} & 0 & 0 & 0 \\ \psi_{1133} & \psi_{2233} & \psi_{3333} & 0 & 0 & 0 \\ 0 & 0 & 0 & \psi_{1212} & 0 & 0 \\ 0 & 0 & 0 & 0 & \psi_{1313} & 0 \\ 0 & 0 & 0 & 0 & 0 & \psi_{2323} \end{pmatrix} \begin{pmatrix} \bar{S}_{11} \\ \bar{S}_{22} \\ \bar{S}_{33} \\ \bar{S}_{12} \\ \bar{S}_{13} \\ \bar{S}_{23} \end{pmatrix}$$

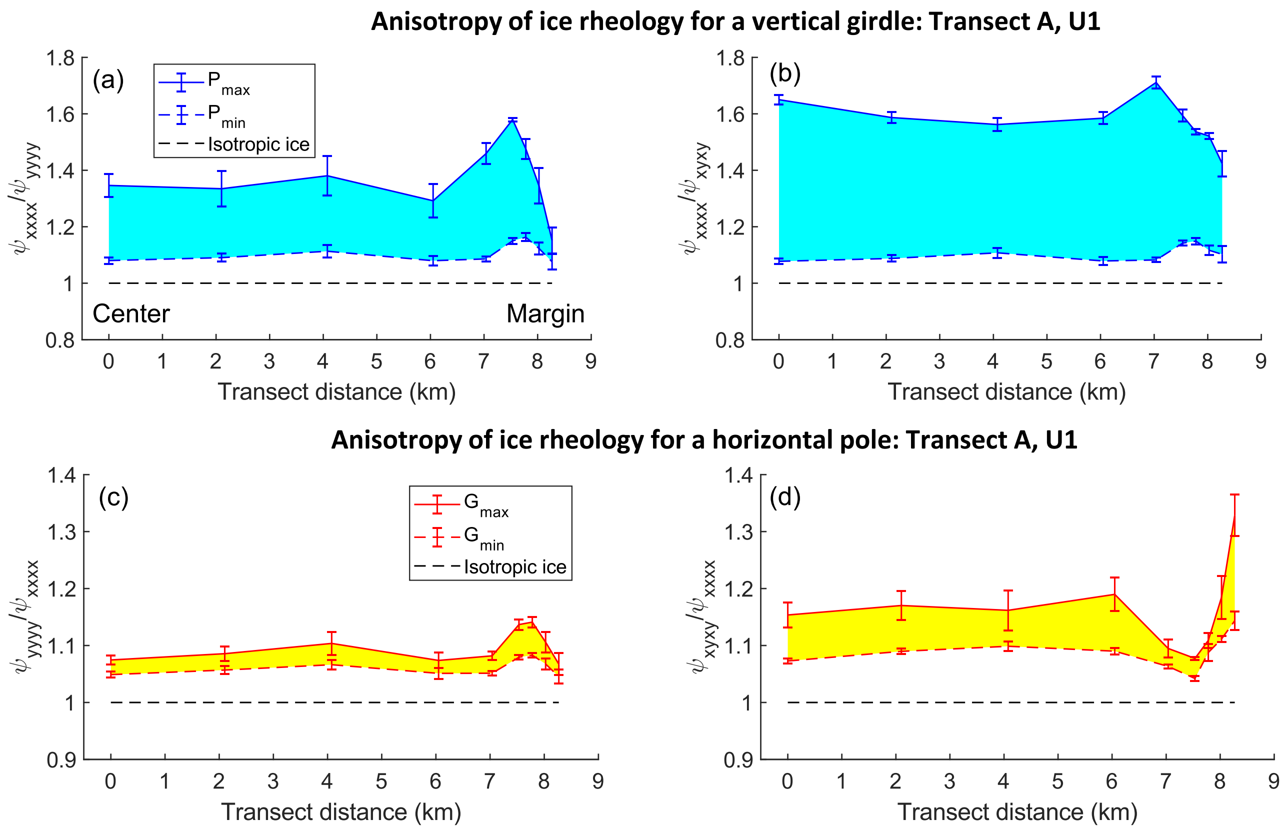

Further reading: Jordan et al. (*in review*) JGR

Application: ARA Neutrino Detection

Because Cherenkov radiation occurs within applicable radar frequencies (~150 – 800 MHz), the effective medium model can be repurposed to model oblique propagation delay and aid neutrino energy reconstruction

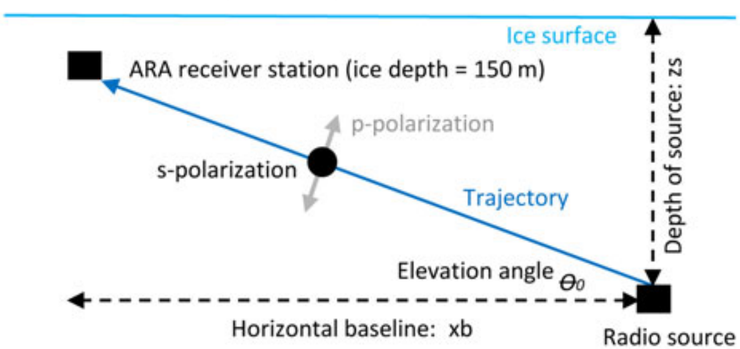

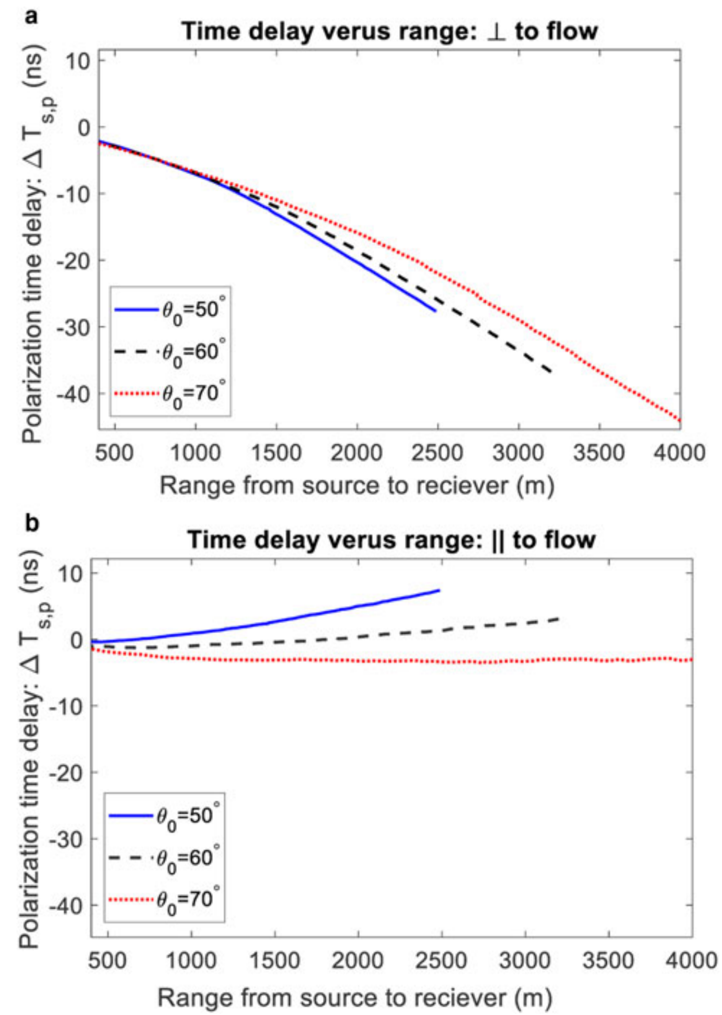

Further reading: Jordan et al. (2020) AoG

Proposals for future work at South Pole

- Quantifying depth-space variations in fabric strength and orientation across IceCube domain
- Generalising Jordan et al. (2020)'s model framework for neutrino detection for off-axis alignment
- Bistatic radar surveys to resolve a_3
- Anisotropic flow parameterisation and modelling of South Pole domain